

# The lasercom test and evaluation station for flight terminal evaluation

K. E. Wilson, N. Page, A. Biswas, H. Hemmati,  
K. Masters, J. Erickson and J. R. Lesh,

Jet Propulsion Laboratory  
California Institute of Technology  
4800 Oak Grove Dr.  
Pasadena, CA 91109-8099

## ABSTRACT

Full-up pre-launch characterization of a lasercom terminal's communications and acquisition/tracking subsystems can provide quantitative characterization of the terminal and better realize the benefits of any demonstration. The lasercom test and evaluation station (LTES) being developed at NASA/JPL is a high quality optical system that will measure the key characteristics of lasercom terminals that operate over the visible and near-infrared spectral region. The LTES's large receiving aperture will accommodate terminals up to 20 cm. in diameter. The unit has six optical channels and it measures far-field beam pattern, divergence, data rates up to 1.4 Gbps and bit-error rates as low as  $10^{-9}$ . It also measures the output power of the laser-terminal's beacon and communications channels. The 1 kHz frame rate camera in LTES's acquisition channel measures the point-ahead angle of the laser communications terminal to a resolution of 1  $\mu$ rad. When combined with the data channel detection, the acquisition channel measures acquisition and reacquisition times with a 1 ms resolution.

Keywords: Laser terminal, optical, lasercom, laser transmitter, divergence, testbed

## 1. INTRODUCTION

Recent successful demonstrations of laser communications with spacecraft and Earth-orbiting satellites have demonstrated the feasibility of some of the key aspects of this technology. Principally, the demonstrations have shown the ability to point a narrow laser beacon from a ground station to a spacecraft in deep-space<sup>1</sup> and the ability to perform high data rate bi-directional communications with a satellite both at night and during the day<sup>2,3</sup>. As the number of optical communications experiments increase, we expect that the lasercom test and evaluation station (LTES) and like instruments to be routinely used to characterize the pre-launch performance of the various laser communications terminals. By establishing a basic set of quantitative tests of the various terminal functions, experimenters would be better able to compare pre-launch and on-orbit performance of different terminals and to more fully realize the benefits of the experiments.

The LTES currently under development at NASA/JPL was initially conceived to support testing of JPL's 10 cm aperture Optical Communications Demonstrator (OCD)<sup>5,6</sup>. However, it was designed to have the capability to evaluate the performance of essentially any laser communications terminal (LCT) with a transmission aperture up to 20 cm in diameter. The LTES is a high quality optical instrument that can measure the far-field beam divergence and beam profile of the laser communications terminal under test. In the beacon-transmit mode, the LTES emits a near-uniform-intensity laser beam that can be used to characterize the LCT's acquisition/tracking subsystem. It measures acquisition and re-acquisition times to 1 msec accuracy for a range of beacon-laser power levels and for various off-axis angles. It measures the LCT's output power, and bit-error rates on modulated data streams as low as  $10^{-9}$  at data rates up to 1.4 Gbps.

Although the LCT is only a few meters away, the LTES measurements are made in the focal plane of its array detectors, thereby simulating the far field of the LCT<sup>7</sup>. It is designed to operate (upon minimal modification) over the 500 nm - 2000 nm spectral range and it can measure either downlink or simulated uplink beacon wavelengths over this range to an

accuracy of 0.01 nm. To achieve operation over this expanded spectral range, we have used protected-aluminum reflecting surfaces and fused silica and quartz refracting elements for the key components in the optical train. As currently assembled with its silicon detectors, the unit will support LCT characterization in the 0.5 to 1.0  $\mu\text{m}$  spectral region.

The basic LTES unit consists of a transportable 1.6-m x 1-m optical table and two racks of electronic support equipment. It is compact, and can be readily transported to a spacecraft assembly area to allow post-spacecraft-integration testing of the LCT's performance. The LTES will also have the capability of performing dynamic testing of LCT's of less than 20 kg mass. For these tests, the LCT is mounted on a spacecraft simulator platform. The platform is made by Micro Slides Inc. and uses a Compumotor dual axis micro-stepper control. It can rotate 360 degree with a step resolution of 3.4 micro radians. Although the platform is normally mounted so that the horizontal axis rotates, minor modifications accommodate stage rotation about any axis. To characterize the LCT's acquisition and tracking characteristics, the platform will be rotated over small arcs (<10 milliradians) at frequencies up to 20 Hz.

This paper describes the basic LTES unit and its operation. In Section 2, we describe the LTES optical train with its detection electronics and discuss the performance of each of the six channels. Conclusions along with our future plans for testing lasercom terminals, acknowledgments, and references are in Sections 3, 4, and 5, respectively

## 2. THE LTES OPTICAL TRAIN

Developed under an aggressive schedule the LTES was assembled using several off-the-shelf optical and mechanical components. Its optical layout consists of five optical receiving and one optical transmission channel.

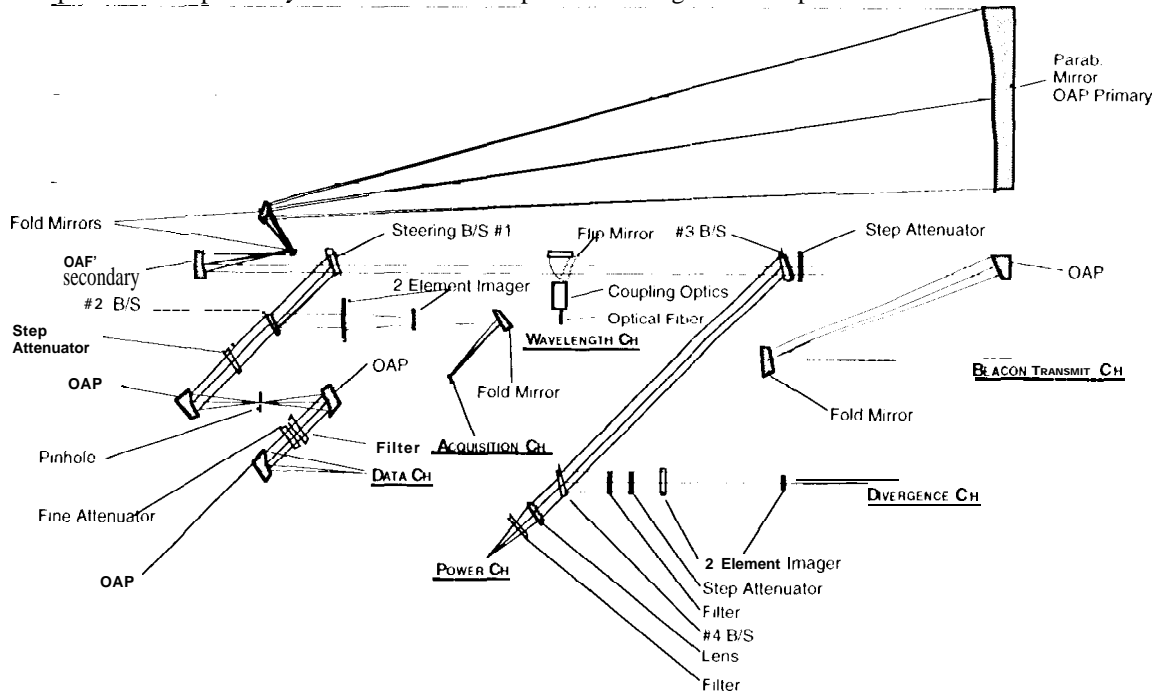


Figure 2.1: LTES optical layout showing the five receiving channels and one beacon transmit channel,

These are the acquisition, the data, the power, the divergence, the wavelength and the beacon-transmit channels, and they are shown in the detailed layout of the LTES optical train of Figure 2.1. The wavefront quality designed for the optical channels was determined by the required image quality needed at the focal plane of the channel. The divergence channel has the highest and the power channel the lowest. We used a Zygo interferometer and a retro-reflecting sphere to align the optical elements and to validate the wavefront quality in each of the optical channels. The interferometer emitted a spatially filtered 10 cm diameter, plane wave He-Ne beam. A picture of the unit with one of its instrument racks is shown in Figure 2.2. The optical table in the figure shows the Space Optics Research Labs (SORL) 20 cm primary mirror, the secondary mirror, the SORL off-axis parabolas (OAPs) for the data and beacon channels, and the data, the acquisition and the divergence channel detectors. Also shown is one of the instrument racks with (from top to bottom) the digital oscilloscope,

the control computer's monitor display, the beam-steering mirror's control electronics, the bit error rate transmitter and receiver, and the control computer.

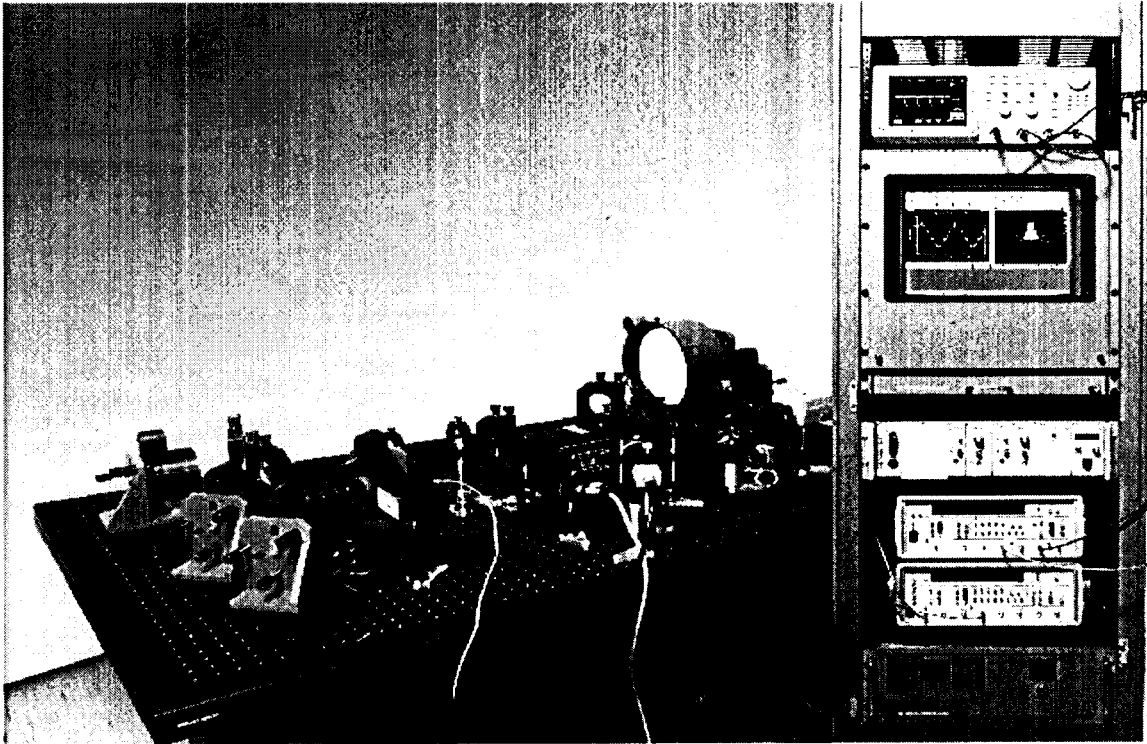


Figure 2.2: Picture of LTES showing the optical bench and one of its two instrument racks. From top to bottom the rack holds the digital oscilloscope, the control computer's monitor display, the beam-steering mirror's control electronics, the bit error rate transmitter and receiver, and the control computer.

There are no obscurations along the LTES's optical train. The telescope is a 10-X afocal reducer with a 20 cm aperture off-axis parabola (OAP) primary mirror that is coupled to an OAP secondary using a pair of fold mirrors. The confocal parabola arrangement provides coma-free performance over the small operating field-of-view, and the two fold mirrors provide beam clearance to the steering beamsplitter gimbal mechanism. The off-axis angles for the parabolas are the same so that the optical beams entering the telescope primary are parallel with those leaving the secondary mirror.

Dielectric coated beamsplitters are used to split the incoming energy off to each channel. The steering B/S #1, the first beamsplitter after the afocal telescope, separates the acquisition and data channels from the remaining four channels. This beamsplitter is mounted in a precision two-axis gimbal-mirror mount with piezoelectric control for fine adjustment. This arrangement enables accurate measurements of the point-ahead angle. The model P-173 piezoelectric translators and model 11-455.20 gimbal-mirror mount were purchased from Physik Instrument. The translators have an angular resolution of 0.276 arc-sec/volt with a maximum tilt angle in both axes of 276 arc-sec. Position sensors along each translational axis reduce the effects of hysteresis and improve the positioning accuracy of the translators.

## 2.1 Data channel

In the data channel the beam reflected from the data/acquisition beamsplitter (#2B/S) is again reflected from a series of three off-axis parabolic mirrors before detection by the high speed data detector. The first parabolic mirror focuses the beam onto a pinhole. The pinhole also helps reject unwanted out-of-field radiation. It also limits the field-of-view of the data channel detector and serves as a reference to validate the performance of the LTES's acquisition system. The light passing through the pinhole is collimated by the second off-axis parabolic mirror. A third off-axis parabola images the beam onto the high speed detector. Coarse (neutral density filters) and fine (waveplate and quartz polarizer) attenuators are used to control the beam power at the detector. The attenuators are placed in the collimated sections of the beam to minimize wavefront distortion. Reducing the aberrations reduces the size of the focused spot and ensures that all of the power is focused onto

the small high-speed detectors that support gigabits per second data rates. We used the Zygo interferometer as a source and measured a  $1/e^2$  spot size of  $40\ \mu\text{m}$  at the position of the detector.

The PIN detectors used in the data channel are the New Focus Model 160 I silicon photodiode with spectral response from 350 nm - 1000 nm and the Model 16 I I germanium photodiode with spectral response from 750 nm - 1800 nm. The detectors have an active area of  $400\ \mu\text{m} \times 400\ \mu\text{m}$ , and  $100\ \mu\text{m} \times 100\ \mu\text{m}$ , respectively. The 3 dB bandwidth limits of these detectors are 25 kHz and 1 GHz. The noise equivalent powers are  $25\ \text{pW}/\sqrt{\text{Hz}}$  for the Model 1601 and  $17\ \text{pW}/\sqrt{\text{Hz}}$  for the Model 1611.

## 2.2 Acquisition channel

The acquisition channel consists of a simple two-element lens pair, a folding mirror, and a high framing rate Adaptive Optics Associates CCD camera. The collimated beam exiting the afocal telescope is reflected first by the steering beamsplitter and then by the data/acquisition beamsplitter into the two-element refracting imaging lens system of the acquisition channel. The two element imaging lens system has a 2:1 telephoto ratio and yields a reasonably well corrected flat field image. The effective focal length of this channel is  $4.13\ \text{m} \pm 1\%$  at 633 nm. Residual aberrations are primarily simple third order spherical and are less than 0.1 waves P-V (peak-to-valley) on-axis, and less than 0.3 waves P-V over the field of view.

The acquisition detector is a  $256 \times 256$  element CCD camera with  $16\ \mu\text{m} \times 16\ \mu\text{m}$  square pixels. The LCT beam is defocused at the acquisition camera to allow 1 prad accuracy in beam-centroid determination while allowing point-ahead angle measurement up to 200 prad. The camera's frame-grabber board located in the acquisition computer is capable of storing 4096 full frames of data. Upon enabling frame acquisition at a specified rate, the buffer is updated in real time as the frames are acquired. After receiving an external trigger, a pre-determined number of pre-trigger and post-trigger frames are captured in the buffer and transferred to the hard disk drive of the acquisition computer on demand. Stored data are processed using IDL image processing routines to yield pixel coordinates of the laser spot's centroid. Time tagged data files containing frame number and centroid coordinates are transferred to the master computer and collated with other LTES data.

## 2.3 Divergence channel

LTES measures the far-field beam-intensity profile which is located at the focal plane of the divergence channel (see Figure 2.1). The LCT beam transmitted by the steering beamsplitter is reflected by a dichroic beamsplitter, #3B/S, that reflects 98% of the incident beam at the LCT wavelength. In the current design this is 844 nm. The beam incident on the divergence/power channel beamsplitter #4B/S is reflected by a 35% reflection beamsplitter into a two element divergence channel imaging lens system and onto a Cohu 4810 camera. The two element imager lens system provides a well-corrected image at the detector. The residual aberrations in this channel were measured as 0.044 waves P-V (633 nm) of third order spherical across the field-of view.

The Cohu camera is operated using a frame grabber board and software supplied by Spirocon. The "Ultracal" feature of the software improves the rejection of the CCD dark noise enhancing the quality of the far-field patterns of the LCT beam profiles. Preliminary test results with the Zygo interferometer's output show that 82% of the beam energy was within the first dark ring. This is shown in Figure 2.3 along with the beam profile for an unaberrated ( $\text{Strehl} = 1$ ) optical system. These results corroborate our wavefront measurements for this channel. Over a 10 cm aperture the Strehl ratio in the LTES's divergence channel exceeds  $0.95^{89}$ .

Depending on the application, the divergence of optical beams has been defined as either the full-width of the beam at the  $1/e^2$  intensity or the full-width of the beam at half the maximum intensity (FWHM). In either definition, an accurate determination of the beam divergence from a measurement of spot size at the focus requires an accurate knowledge of the focal length of the focusing system. Because of this sensitivity, we have designed the divergence channel to be slow,  $f/72$  with full 20 cm aperture illumination. We used the knife-edge method to determine the location of the focus in the divergence channel. The measured effective focal length was  $14.42\ \text{m} \pm 1\%$  for 633 nm light. We used Code-V software to calculate the focal length shift caused by the dispersion in the refractive index of the refracting elements for the OCD's operating wavelength. The calculated focal length was  $14.45\ \text{m}$  at 844 nm within the uncertainty of our measurement.

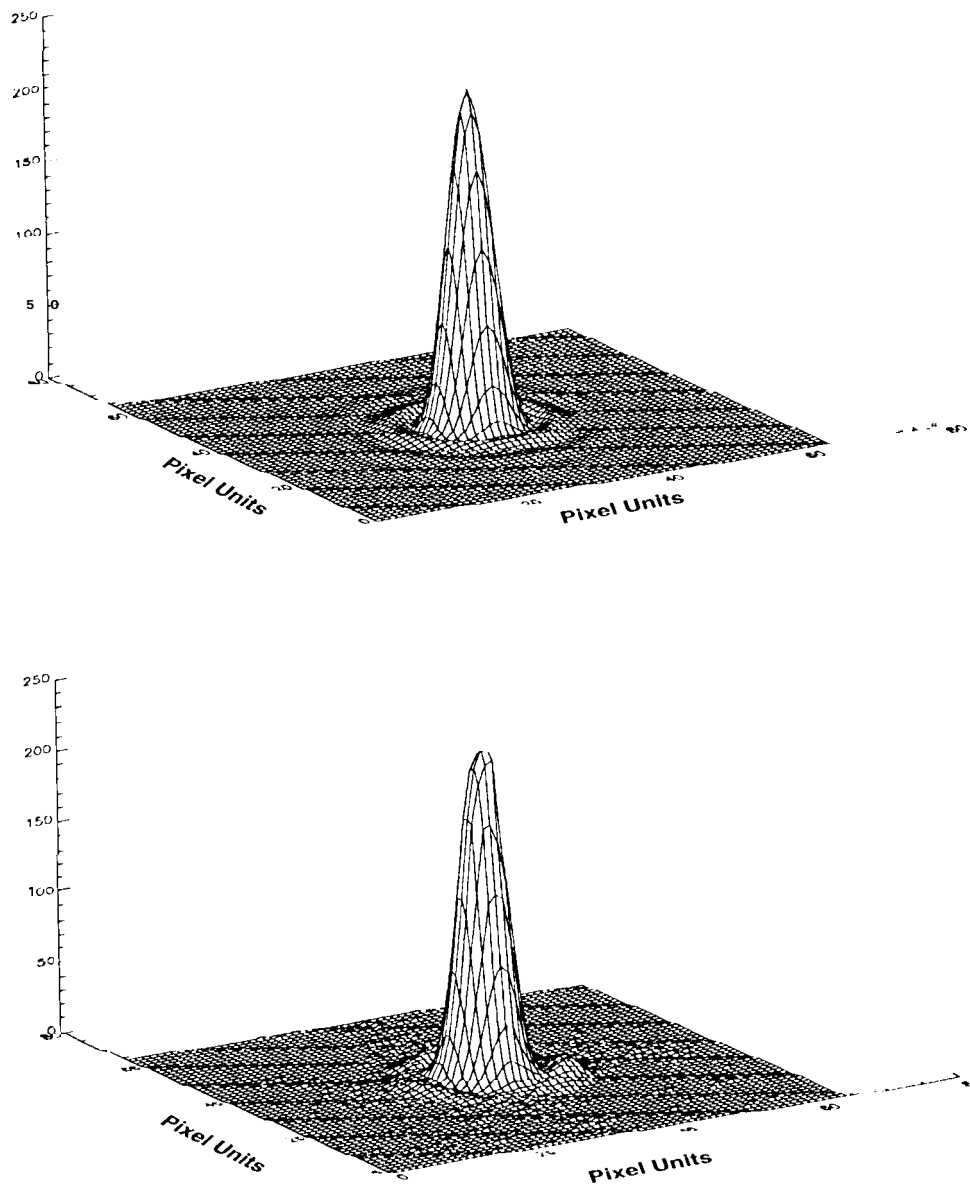


Figure 2.3: The upper picture is the Airy's disk pattern for a 10 cm apertured plane wave in an unaberrated system ( $|\text{Strehl}| = 1$ ). The lower picture is the beam profile of the Zygo beam taken with the Spirocon camera in the acquisition channel ( $\text{Strehl} > 0.95$ ). The two beams profiles have been normalized to the same energy. The energy enclosed in the first dark ring of the upper picture is 840A, that in the lower picture is 82%.

## 2.4 Power channel

The I.C.T signal transmitted through the 50/50 beamsplitter in the power/divergence channel is then incident on a simple single-element plano-convex lens that focuses it onto the power meter, (see Figure 2.1). Because these photodetectors are large area devices, there were no requirements on the optical beam quality in this channel. We estimate that the aberration

in this channel is about 4 waves of simple third-order spherical at 633 nm. The focused spot is much smaller than the power meter's diameter.

An Anritsu model MI9107I optical power meter is used to measure the optical power. We use the model MA9802A silicon photodiode sensor head for measurements in the visible and near-IR spectral region (0.35 - 1.15  $\mu\text{m}$ ). This photodiode has a 9.5 mm diameter photosensitive surface, and a dynamic range of -65 dBm to +20 dBm with 0.01 dB resolution. For the longer wavelengths, we use the model MA9302A germanium photodiode. This detector has a 5 mm diameter photosensitive surface with a dynamic range of -40 dBm to +20 dBm with a 0.01 dB resolution.

## 2.5 Wavelength channel

The LTES uses a Burleigh model WA-1000 wavemeter to measure the wavelengths of the LCT and LTES beacons. The wavemeter measures wavelengths by counting the interference fringes produced by the input beam in a Michelson interferometer. It compares these with fringes produced in the same Michelson by a stabilized He-Ne light source.

The beam in the LTES is coupled into the WA-1000 using the flip mirror located as shown in Figure 2.1. This reflects the laser beam to a 30-times beam reducer. Depending on the wavelength of the unit under test, the output of the reducer is either coupled into a focusing lens and then into a single mode fiber or is directly coupled to the free-beam input aperture of the WA-1000. Wavelengths are measured to an accuracy of 0.01 nm, and appropriate beamsplitters and detectors are replaced into the wavemeter's optical path to measure probe wavelengths in indifferent regions of the spectrum.

## 2.6 Beacon transmit channel

The beacon transmit channel is shown in Figure 2.1. The LTES beacon serves as a reference for the LCT's acquisition and tracking subsystem. The beacon laser's output is coupled to the optical train using a single mode fiber. A fold mirror directs the beam emitted by the fiber to the off-axis parabolic mirror that collimates the beam. The collimated beam passes through a dichroic beamsplitter that transmits >95% of the incident 780 nm beacon power and reflects >95% of the light at the 844 nm OCD's emission wavelength. After the dichroic beamsplitter the beacon light is coupled to the afocal telescope where it is expanded to 20 cm., maintaining less than 0.2 dB center-to-edge variation in beam intensity across the aperture to simulate a uniform intensity plane wavefront.

## 3. CONCLUSION

We have described the laser terminal evaluation station currently under development at JPL. The LTES will be first used to test the OCD. The OCD's system architecture consists of three channels, a transmit channel, a receive channel and a boresite channel. The transmitter is a 10-cm-aperture Cassegrain telescope with a CCD array in the focal plane to acquire and track the uplink beacon. A dual-axis fine-pointing mirror reduces the effects of platform disturbances and enables the terminal to achieve the required point-ahead angle of its transmitted beam. In the beacon-transmit mode LTES will transmit a  $780 \pm 3$  nm laser beacon signal to the OCD and the OCD in turn transmits back an  $844 \pm 1$  nm modulated laser signal to the LTES. The LTES will be used to measure the Strehl of the OCD's transmit channel and validate the field-of-view of the boresite channel designed at 200  $\mu\text{rad}$ .

## 4. ACKNOWLEDGMENTS

We would like to acknowledge the technical assistance of Drs. T. Yan, C. Chen, and S. Myau during the initial design phase of the LTES, Mr. J. Packard for technical assistance, and Mr. F. Razo of JPL's Measurement Technology Center for writing the instrument control and data collection software. We would also like to thank Dr. E. Baroth of the Measurement Technology Center for his guidance and many fruitful discussions.

The research described in this paper was carried out at the Jet propulsion laboratory, California Institute of Technology, under a contract with the National Aeronautics and Space Administration.

## 5. REFERENCES

1. K. F. Wilson and J. R. Lesh, "GOPEX: A Laser Uplink to the Galileo Spacecraft on its Way to Jupiter," SPIE Proceedings, vol. 1866, pp. 138-147, Jan. 1993.

2. K. E. Wilson, M. Jeganathan, J. James, G Xu, and J. R. Lesh, "Results form Phase-1 and Phase-2 GOLD Experiments", JPL TDA Progress Report 42-127, November IS, 1996.
3. Y. Arimoto et al. "Preliminary result on Laser Communication Experiment Using [11'S-VI" Photonics West '95, Free-Space Laser Communication Technologies VIII, Feb. 1995.
4. C.-C. Chen and J. K. Lesh, "Overview of the Optical Communications Demonstrator," Proceedings of SPIE Vol. 2123 pp. 85-95, Los Angeles, CA, January 1994.
5. N. Page, "Design of the Optical Communication Demonstrator Instrument Optical System," Proceedings of SPIE Vol. 2123, pp. 498-504 Los Angeles, CA, January 1994.
6. J1. Hemmati and D. J. Copeland, "Laser Transmitter Assembly for Optical Communications Demonstrator," Proceedings of SPIE Vol. 2123 pp. 283-291, Los Angeles, CA, January 1994.
7. K. Inagaki et al. "Far-field measurement of on-board laser Communication Equipment by free-space transmission simulator" Proceedings of SPIE Vol. 1866 pp. 83 - 94 Los Angeles, CA, January 1993.
8. M. Born and E. Wolf, *Principles of Optics*, p. 398. (Pergamon Press, Oxford, Fifth Edition 1975).
9. W. J. Smith, *Modern Optical Engineering*, p. 337. (McGraw- Hill, New York, Second Edition, 1990).